Journal of Materials Chemistry A

Accepted Manuscript

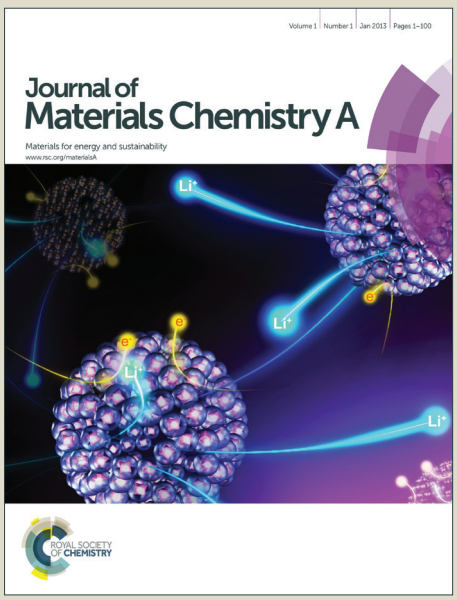

ROYAL SOCIETY OF CHEMISTRY

www.rsc.org/materialsA

Journal Name

COMMUNICATION

Porous Cobalt-Nitrogen-Doped Hollow Graphene Spheres as Superior Electrocatalyst for Enhanced Oxygen Reduction in both Alkaline and Acidic Solutions

Received 00th January 20xx,
Accepted 00th January 20xx

DOI: 10.1039/x0xx00000x

www.rsc.org/

Qiangmin Yu,[abc] Jiaoxing Xu,[ab] Chunying Wan,[abc] Chuxin Wu,[ab] and Lunhui Guan*[ab]

Porous cobalt-nitrogen-doped hollow graphene spheres were prepared by template synthesis method. As the catalyst for oxygen reduction reaction, they exhibit excellent electrocatalytic activity, superior methanol tolerance and strong durability not only in alkaline solution, but also in acidic solution. The unprecedented electrocatalytic performance of the catalyst is attributed to the well-defined morphology, high specific surface area (321 m^2/g), large pore volume (1.8 cm^3/g) and homogeneous distribution of cobalt-nitrogen active sites.

The oxygen reduction reaction (ORR) has been regarded as a key to control the performance of fuel cells, but it suffers from sluggish kinetics.[1, 2] Exploring new electrocatalysts to improve the ORR activity becomes hot issues. The activity of electrocatalysts for ORR mainly depend on the electron transfer process, crossover effect and long-term stability. Currently, Pt-based catalysts have been used to catalyze the ORR with a high efficiency.[3, 4] However, the high cost, the time dependent drift, and the low tolerance to methanol of the Pt-based catalysts are still big obstacles for the commercialization of fuel cells.[5] Therefore, numerous efforts have been devoted to reducing or substituting Pt-based catalysts by employing non-precious metal catalysts and heteroatom-doped carbonaceous materials. Advanced carbon materials with ordered graphitic structures including carbon nanotubes (CNTs), carbon nanofibers (CNFs), onion-like carbon and graphene have been studies as electrocatalysts due to their unique surface structures, high electric conductivity, large surface area and environmental friendliness.[6] For instance,the vertically aligned nitrogen-doped carbon nanotube arrays exhibited excellent electrocatalytic activity for ORR.[7] Co_3O_4 nanocrystals on graphene as a synergistic catalyst exhibited highly active for ORR in alkaline solution.[8]

Nitrogen-coordinated metals supported on carbon nanomaterials (M-N-C) have been explored as new catalyst for ORR.[9-11] Very recently, the Fe-N-doped carbon nanofibers catalyst reported by Yu *et al* showed outstanding ORR activity comparable to Pt/C catalyst in alkaline media, but poor in acidic media.[12] As we know, A new catalyst with excellent ORR performance in acidic environments is desired because most fuel cells operate in acidic electrolytes.[13] However, most nanocarbon-based catalysts exhibited high performance of ORR activity in alkaline media, but poor activity in acids due to the effects of catalyst structure.[14-16] It is emergent to develop carbon-based catalysts with both optimal activity and stability for ORR in acidic solutions.

Herein, on the basis of well-defined morphology and efficient electron transfer, we report a facile, scalable approach for fabricating a cobalt-nitrogen-doped hollow graphene sphere (Co-N/HGS) catalyst. The Co-N/HGS catalyst with a well-defined geometry, high surface area, large pore volume and high nitrogen content, exhibits highly efficient electrocatalytic activity and superior stability for ORR not only in alkaline but also in acidic environments.

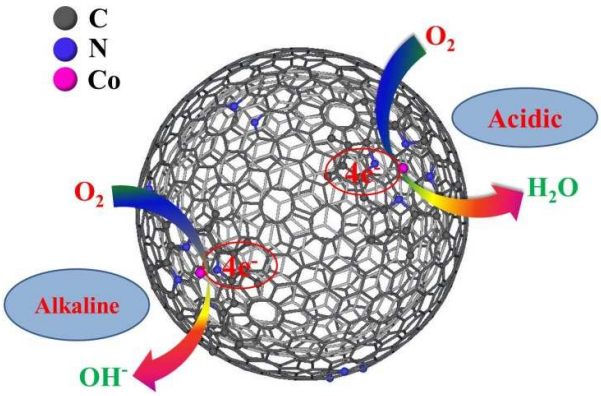

Scheme 1. Schematic presentations showed the ORR on the envisaged microstructures of Co-N/HGS.

[a] *Key Laboratory of Design and Assembly of Functional Nanostructures, Fujian Institute of Research on the Structure of Matter, Chinese Academy of Sciences, YangQiao West Road 155#, Fuzhou, Fujian 350002, P.R. China. Fax: (+) 86-591-6317 3550; Tel: 86-591-6317 3550 E-mail: guanlh@fjirsm.ac.cn*
[b] *Fujian Key Laboratory of Nanomertials, Fuzhou, Fujian 350002, China*
[c] *University of Chinese academy of sciences, Beijing 100049, China*
† Footnotes relating to the title and/or authors should appear here.
Electronic Supplementary Information (ESI) available: [details of any supplementary information available should be included here]. See DOI: 10.1039/x0xx00000x

Co-N/HGSs were synthesized by template method. The overall synthesis procedure is schematically illustrated in Scheme S1. Briefly, silica templates were coated with graphene oxide through surface modification. The solid products were heated in a nitrogen atmosphere at 850 ℃ for 2h and then etched by HF (10 wt. %) solutions. The hollow graphene spheres (HGSs) were formed after dried. It should be noted that the diameter of the HGS was completely controlled by the silica template. Thus, a number of HGSs with different diameters were synthesized and characterized as the comparative samples (see Supporting Information for more details). The HGSs with diameter of 300 nm have the best morphology, thus they were chosen for the following experiments. Finally, the HGSs were dispersed in Vitamin B12 solution under stirring before filtration. The obtained solid composites were then pyrolysis at 700℃ under nitrogen atmosphere for 3 h, and the Co-N/HGS catalysts were formed. For comparison, cobalt-nitrogen-doped active carbon (Co-N/AC) and reduced graphene oxide nanosheet (Co-N/RGO) were synthesized under the same procedure.

Nitrogen physisportion of Co-N/HGS was first measured to investigate the porous structure (**Figure 1a**). The Brunauer-Emmett-Teller surface areas of the Co-N/HGS are 321 m^2/g. The corresponding pore size distributions (inserted image) suggest that the diameters of the pores are in the range of 4 to 35 nm. The pore volume is 1.8 cm^3/g, very favorable for mass transfer. The microstructure of the obtained materials were examined by scanning electron microscopy (SEM) and transmission electron microscopy (TEM). Typical TEM image (**Figure 1b**) of some Co-N/HGS indicates that the quite uniform spheres with a diameter of 300 nm interlink with each other. It should be noted that the morphology of Co-N/HGS kept intact after electrode preparation. HR-TEM image (**inserted in Figure 1c**) demonstrates a distance of 0.35 nm, corresponding to the interlayer stacking of reduced graphene oxide nanosheets. Moreover, elemental mapping of the Co-N/HGS illustrates a homogeneous distribution of C, N and Co atoms in the hollow graphene spheres (**Figure 1d**).

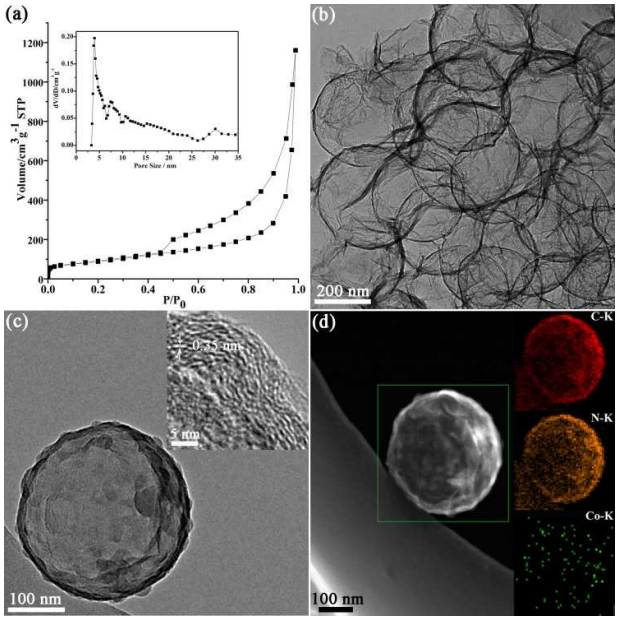

Figure 1. (a) Nitrogen sorption isotherm and pore size distribution (inserted image) of Co-N/HGS. (b), (c) TEM and HR-TEM (inserted) images of Co-N/HGS. (d) Scanning transmission electron microscopy (STEM) image of Co-N/HGS and the corresponding element mapping images (inserted) of carbon, nitrogen and cobalt.

X-ray photoelectron spectroscopy (XPS) analysis double-checked the presence of C, N, O and Co in the Co-N/HGS catalyst (**Figure 2a**). The nitrogen and cobalt content of the Co-N/HGS was 6.30% and 0.51% examined by XPS analysis. The high-resolution N 1s spectrum of the Co-N/HGS catalyst shows two dominant nitrogen peaks at 400.6 eV and 398.5 eV (**Figure 2b**), assigned to pyrrolic N and pyridinic N.[17, 18] The peak at 398.5 eV should also include a contribution from nitrogen bound to the metal (M-N), due to the small difference between binding energies of N-Me and pyridinic N.[17, 19] Pyridinic N (probably including M-N) is generally believed to participate in the active sites for ORR.[17, 19, 20] The high-resolution O 1s spectrum is deconvoluted into two peaks with binding energies of 533.1 and 531.4 eV (**Figure 2c**), which can be assigned to metal-bound oxygen and C=O (aldehydes, ketones, lactones), respectively.[21] In the Co 2p spectrum (**Figure 2d**), the peaks at 780.2 and 785.8 eV are assigned to Co-N species, while the peaks at 796 and 801.7 eV originate from Co-O species.[22] It is well-known that the metal-oxygen sites have been reported to be inactive for ORR in acidic media.[22] Thus, the activity of the Co-N/HGS in acid solution was mainly ascribed to Co-N species. It should be noted that the nitrogen and cobalt content remained almost the same for the Co-N/AC (6.08% and 0.5%) and Co-N/RGO

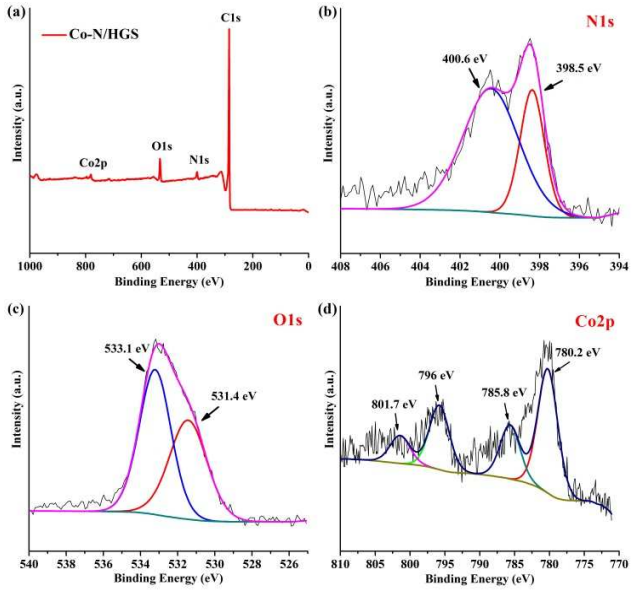

Figure 2. (a) The XPS survey spectra (0-1000 eV) of Co-N/HGS. (b) High-resolution N 1s spectrum. (c) High-resolution O 1s spectrum. (d) High-resolution Co 2p spectrum.

(5.83% and 0.48%) (**Figure S3**), indicating that doping Co-N with VB 12 is effective for all the carbon nanomaterials.

The cathodic ORR electrocatalytic properties of the Co-N/HGS electrode were tested in a three-electrode system at room temperature. **Figure 3a** shows the cyclic voltammogram (CV) curves of the Co-N/HGS electrode in N_2- and O_2-saturated aqueous solution of 0.1 M NaOH at a scan rate of 50 mV s^{-1}, respectively. As compared to no reduction peak in the N_2-saturated solution, a pronounced reduction peak at -0.12 V in the O_2-saturated solution indicates the electrocatalytic activity of the Co-N/HGS for the ORR.

To further investigate the ORR electrocatalytic activity of Co-N/HGS, we carried out the linear sweep voltammetry (LSV) measurements on a rotating disk electrode (RDE) for each of the electrode materials, including the HGS, Co-N/RGO, Co-N/AC and commercial 20 wt% Pt/C electrodes, in O_2-saturated 0.1 M NaOH solution at a scan rate of 10 mV/s and a rotation rate of 1600 rpm (**Figure 3b**). The catalytic parameters for the ORR are summarized in **Table 1**. The ORR activity of the Co-N/HGS electrode is actually even better than that of commercial Pt/C. It displays a more positive onset potential (0.04 V) than that of HGS (-0.15 V), Co-N/RGO (-0.09 V), Co-N/AC (-0.07 V) and Pt/C (0.02 V). In addition, Co-N/HGS showed a more positive half-wave potential ($E_{1/2}$ = -0.07 V) and high diffusion-limiting current (-6.3 mA cm^{-2}), superior to half-wave potential (-0.12 V) and diffusion-limiting current (-5.71 mA cm^{-2}) of the Pt/C (**Figure 3b**). RDE experiments at different rotating speeds were carried out (**Figure 3c**) to measure the kinetic parameters,

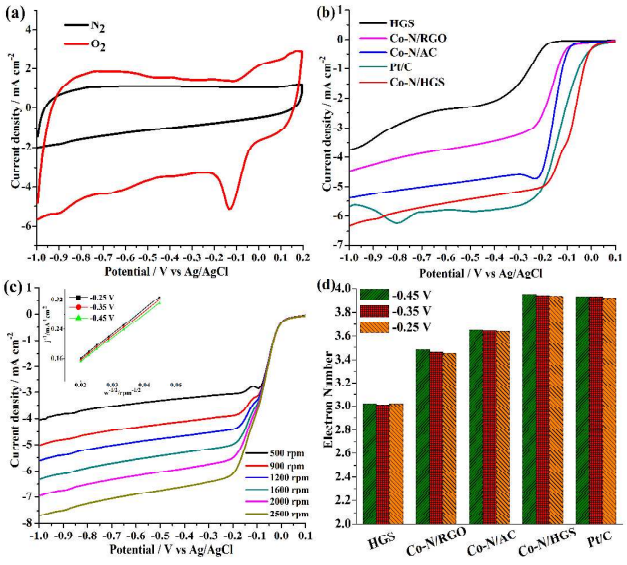

Figure 3. (a) Cyclic voltammograms of the Co-N/HGS at a scan rate of 50 mV s^{-1} in 0.1 M NaOH solution saturated with N_2 and O_2. (b) Linear sweep voltammetry (LSV) curves for the HGS, Co-N/RGO, Co-N/AC, Co-N/HGS and Pt/C electrode in O_2-saturated 0.1 M NaOH at 10 mV s^{-1} (from positive to negative) at 1600 rpm. (c) LSV curves for the Co-N/HGS electrode at different rotation rates in O_2-saturated 0.1 M NaOH at 10 mV s^{-1} (from positive to negative). The inset shows the Koutecky-levich (K-L) plot. (d) The n values of the HGS, Co-N/RGO, Co-N/AC, Co-N/HGS and Pt/C against electrode potential.

Table 1. The ORR performance of different catalysts in alkaline media

Sample	Onset potential (V)[a]	Half wave potential (V)[a]	Diffusion-limiting current (mA/cm^2)	Electron transfer number at -0.3V[a]
HGS	-0.15	-0.27	3.73	3.02
Co-N/RGO	-0.09	-0.17	4.47	3.48
Co-N/AC	-0.07	-0.15	5.36	3.65
Co-N/HGS	0.04	-0.07	6.30	3.96
Pt/C	0.02	-0.12	5.71	3.94

[a] V vs. Ag/AgCl

which were analyzed by the Koutecky-Levich (K-L) equation (**inserted in Figure 3c**). The number of electrons transfer was determined to be 3.93-3.95 (calculated from -0.25 to -0.45 V), indicating that a four-electron pathway dominated the ORR process. In contrast, the HGS, Co-N/RGO and Co-N/AC exhibited much lower n valued of 3.01, 3.46 and 3.65 at -0.35 V, respectively (**Figure 3d**). Most importantly, the Co-N/HGS electrode exhibits highly efficient electrocatalytic activity and superior stability for ORR in acidic solution. The HGS, Co-N/RGO, Co-N/AC, Co-N/HGS and Pt/C electrodes in 0.5 M H_2SO_4 electrolyte were evaluated by RDE measurements (**Figure 4**). The CV curves show no any significant peak in the N_2-saturated electrolyte. On the contrary, a characteristic ORR peak at about 0.47 V (V vs. Ag/AgCl) was observed in the presence of oxygen, indicating the electrocatalytic activity of Co-N/HGS for ORR (Figure 4a). The performance of all catalysts is summarized in **Table 2**. The ORR onset potentials of each sample were acquired from RDE linear sweep at 1600 rpm (**Figure 4b**). Remarkably, the onset potential of the Co-N/HGS electrode is comparable to that of Pt/C (0.67 V vs. Ag/AgCl), and much more positive than the previous carbon-based electrocatalysts in acidic solution ever reported (**Table S1**).[12, 23, 24] More significantly, the current density of the Co-N/HGS electrode are larger than that of Pt/C. The difference on the current density between Co-N/HGS and Pt/C mainly derived from the pore volume and electrical conductivity.

The reaction kinetics was also studied by rotating disk voltammetry. **Figure 4c** presents the voltammetric profiles of the Co-N/HGS electrode in the O_2-saturated 0.5 M H_2SO_4 electrolyte, where the current density enhances with increasing rotation rated (from 500 to 2500 rpm). The inserted image of **Figure 4c** depicts the corresponding Koutecky-Levich plots at various electrode potentials. The data exhibit good linearity, and the slopes remain approximately constant over the potential range from 0.1 to 0.3 V, suggesting an efficient electron transfer process. The number of electrons transfer was calculated to be 3.9-3.92 at 0.3 to 0.1 V, much higher than that of the HGS (~2.75), Co-N/RGO (~3.3) and Co-N/AC (~3.75), and even comparable to Pt/C (~3.94) at 0.2 V (**Figure**

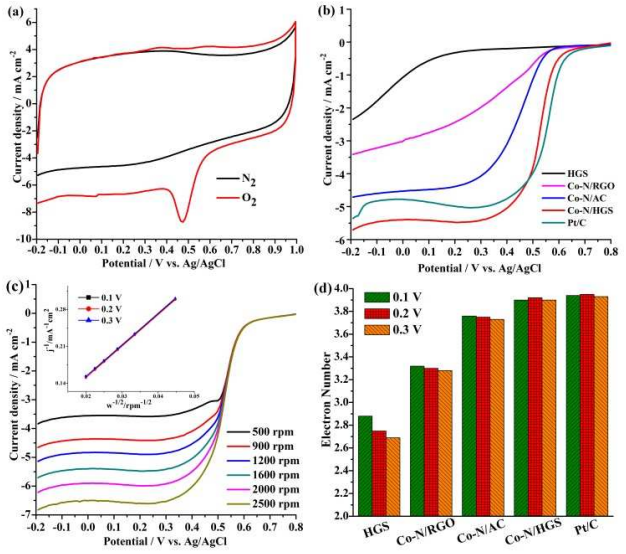

Figure 4. (a) Cyclic voltammograms of the Co-N/HGS electrode at a scan rate of 50 mV s^{-1} in 0.5 M H_2SO_4 solution saturated with N_2 and O_2. (b) Linear sweep voltammetry (LSV) curves for the HGS, Co-N/RGO, Co-N/AC, Co-N/HGS and Pt/C electrode in O_2-saturated 0.5 M H_2SO_4 at 10 mV s^{-1} (from positive to negative) at 1600 rpm. (c) LSV curves for the Co-N/HGS electrode at different rotation rates in O_2-saturated 0.5 M H_2SO_4 at 10 mV s^{-1}(from positive to negative). The inset image shows the Koutecky-levich (K-L) plot. (d) The n values of the HGS, Co-N/RGO, Co-N/AC, Co-N/HGS and Pt/C against electrode potential.

Table 2. The ORR performance of different catalysts in acidic media

Sample	Onset potential (V)[b]	Half wave potential (V)[b]	Diffusion-limiting current (mA/cm^2)	Electron transfer number at 0.3V[b]
HGS	0.25	0.01	2.34	2.70
Co-N/RGO	0.57	0.29	3.42	2.28
Co-N/AC	0.58	0.44	4.71	3.73
Co-N/HGS	0.65	0.53	5.69	3.90
Pt/C	0.67	0.56	5.35	3.93

[b] V vs. Ag/AgCl

4d). The Co-N/HGS catalyst exhibits superior catalytic performance derived from its porous structure and metal-nitrogen active sites.

Recently, some experts paid attention to carbon corrosion for carbon matrix electrocatalysts in fuel cells. It exacerbated if the cathode expericence higher potentials. The cathode potential is markedly higher than the standard potential for carbon oxidation, but the actual rate of carbon oxidation is very low due to intrinsic kinetic limitations.[25]

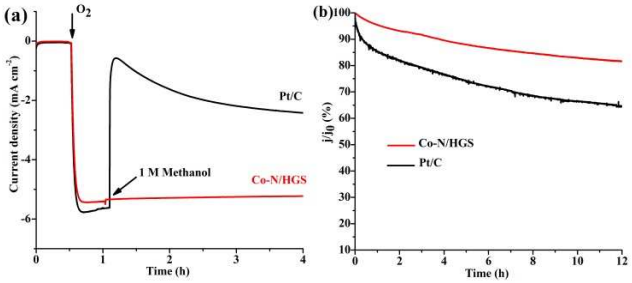

Figure 5. (a) Current-time (i-t) chronoamperometric responses at -0.3 V O_2-saturated 0.1 M NaOH on Co-N/HGS and Pt/C electrode (1600 rpm) followed by introduction of O_2 and methanol (1 M). (b) Current-time chronoamperometric responses at -0.2 V of Co-N/HGS and Pt/C for 12 h in O_2-saturated 0.1 M NaOH solution at a rotation rate of 1600 rpm.

It is well known that fuel molecules (e.g., methanol) could easily cross over through the membrane form anode to cathode. Methanol not only influences the anion exchange membrances, but also poisons the catalyst (Pt/C). Therefore, the tolerance to methanol is a standard for electrochemical performance. The methanol crossover effect was evaluated on both Co-N/HGS and Pt/C electrode (**Figure 5a**). A negative current appeared on both Co-N/HGS and Pt/C when O_2 was introduced to N_2-staurated 0.1 M NaOH solution. After adding 1 M methanol to the electrolyte, as expected, an obvious inversion of the current density was observed for the Pt/C electrode, whereas the Co-N/HGS electrode retained stable response. These results demonstrate the excellent tolerance of the Co-N/HGS electrode to methanol. In addition, the durability of the Co-N/HGS and Pt/C electrode was also assessed through chronoamperometric measurements at -0.2 V for 12 h in an O_2-saturated aqueous solution of 0.1 M NaOH at a rotation rate of 1600 rpm (**Figure 5b**). Remarkably, the corresponding current-time (i-t) chronomaperometric response of Co-N/HGSs exhibits a very low attenuation and a high relative current of 84% still persists after 12 h, whereas Pt/C maintained only 65% of its initial activity in just 12 h. This result clearly suggests the stability of the Co-N/HGS is much better than that of the Pt/C catalyst. Moreover, the durability of the Co-N/HGS and Pt/C in acidic medium (0.5 M H_2SO_4) was also tested at 0.3 V for 12 h. As shown in **Figure S4**, the 12 h test only caused slight activity loss on Co-N/HGS (~18%), whereas Pt/C lost nearly 43% of its initial activity, confirming a much better stability of Co-N/HGS than that of commercial Pt/C in acidic solution. The excellent performance of Co-N/HGS catalyst can be attributed to its unique porous structure. The porous structure enhanced the transport of electrolyte ions, reaction intermediates and products. It might also prevent the dissolution of active sites from hollow graphene sphere matrix.

Conclusions

In summary, we have developed an effective fabrication strategy for generating the Co-N/HGS catalyst by silica templates. The Co-N/HGS catalyst exhibits superior active

activity and excellent electrochemical stability both in alkaline and acidic medium. The outstanding ORR performance of the Co-N/HGS catalyst is inseparable from their well-defined morphology, large pore volume and homogeneous distribution of cobalt-nitrogen active sites. Apart from the use of Co-N/HGS as an electrocatalyst for the ORR, its unique structure and properties indicate their potential for use in other applications such as supercapacitors and batteries.

Acknowledgements

We acknowledge the financial support provided by the National Key Project on Basic Research, the National Natural Science Foundation of China （21101154, 21171163, and 91127020）, the National Key Project on Basic Research (Grant No. 2011CB935904), NSF for Distinguished Young Scholars of Fujian Province (Grant No. 2013J06006).

Notes and references

1. G. Wu, K. L. More, C. M. Johnston and P. Zelenay, *Science*, 2011, 332, 443-447.
2. B. C. H. Steele and A. Heinzel, *Nature*, 2001, 414, 345-352.
3. S. Y. Wang, S. P. Jiang, T. J. White, J. Guo and X. Wang, *J Phys Chem C*, 2009, 113, 18935-18945.
4. H. Yano, J. M. Song, H. Uchida and M. Watanabe, *J Phys Chem C*, 2008, 112, 8372-8380.
5. R. L. Liu, C. von Malotki, L. Arnold, N. Koshino, H. Higashimura, M. Baumgarten and K. Mullen, *J Am Chem Soc*, 2011, 133, 10372-10375.
6. M. Liu, R. Zhang and W. Chen, *Chemical reviews*, 2014, 114, 5117-5160.
7. K. P. Gong, F. Du, Z. H. Xia, M. Durstock and L. M. Dai, *Science*, 2009, 323, 760-764.
8. Y. Liang, Y. Li, H. Wang, J. Zhou, J. Wang, T. Regier and H. Dai, *Nature materials*, 2011, 10, 780-786.
9. M. Lefevre, E. Proietti, F. Jaouen and J. P. Dodelet, *Science*, 2009, 324, 71-74.
10. G. Wu, K. L. More, C. M. Johnston and P. Zelenay, *Science*, 2011, 332, 443-447.
11. B. Su, I. Hatay, A. Trojanek, Z. Samec, T. Khoury, C. P. Gros, J. M. Barbe, A. Daina, P. A. Carrupt and H. H. Girault, *J Am Chem Soc*, 2010, 132, 2655-2662.
12. Z. Y. Wu, X. X. Xu, B. C. Hu, H. W. Liang, Y. Lin, L. F. Chen and S. H. Yu, *Angewandte Chemie*, 2015, DOI: 10.1002/anie.201502173.
13. L. Chen, R. Du, J. Zhu, Y. Mao, C. Xue, N. Zhang, Y. Hou, J. Zhang and T. Yi, *Small*, 2015, 11, 1423-1429.
14. W. Wei, H. Liang, K. Parvez, X. Zhuang, X. Feng and K. Mullen, *Angewandte Chemie*, 2014, 53, 1570-1574.
15. Y. Li, W. Zhou, H. Wang, L. Xie, Y. Liang, F. Wei, J. C. Idrobo, S. J. Pennycook and H. Dai, *Nature nanotechnology*, 2012, 7, 394-400.
16. J. Liang, Y. Jiao, M. Jaroniec and S. Z. Qiao, *Angewandte Chemie*, 2012, 51, 11496-11500.
17. U. Koslowski, I. Herrmann, P. Bogdanoff, C. Barkschat, S. Fiechter, N. Iwata, H. Takahashi and H. Nishikori, *Ecs Transactions*, 2008, 13, 125-141.
18. Y. Nabae, S. Moriya, K. Matsubayashi, S. M. Lyth, M. Malon, L. B. Wu, N. M. Islam, Y. Koshigoe, S. Kuroki, M. A. Kakimoto, S. Miyata and J. Ozaki, *Carbon*, 2010, 48, 2613-2624.
19. G. Wu, C. M. Johnston, N. H. Mack, K. Artyushkova, M. Ferrandon, M. Nelson, J. S. Lezama-Pacheco, S. D. Conradson, K. L. More, D. J. Myers and P. Zelenay, *J Mater Chem*, 2011, 21, 11392-11405.
20. Y. Zhao, K. Watanabe and K. Hashimoto, *J Am Chem Soc*, 2012, 134, 19528-19531.
21. H. T. Chung, J. H. Won and P. Zelenay, *Nature communications*, 2013, 4.
22. G. Wu, Z. W. Chen, K. Artyushkova, F. H. Garzon and P. Zelenay, *Ecs Transactions*, 2008, 16, 159-170.
23. M. Zhou, C. Yang and K.-Y. Chan, *Adv Energy Mater*, 2014, 4, n/a-n/a.
24. Z. S. Wu, L. Chen, J. Liu, K. Parvez, H. Liang, J. Shu, H. Sachdev, R. Graf, X. Feng and K. Mullen, *Adv Mater*, 2014, 26, 1450-1455.
25. J. Parrondo, T. Han, E. Niangar, C. Wang, N. Dale, K. Adjemian and V. Ramani, *Proceedings of the National Academy of Sciences of the United States of America*, 2014, 111, 45-50.